PNAS RESEARCH ARTICLE | NEUROSCIENCE

Propionate exerts neuroprotective and neuroregenerative effects in the peripheral nervous system

Thomas Grüter[a,1], Nuwin Mohamad[a], Niklas Rilke[a], Alina Blusch[a], Melissa Sgodzai[a], Seray Demir[a], Xiomara Pedreiturria[a], Katharina Lemhoefer[a], Barbara Gisevius[a], Aiden Haghikia[a,b], Anna Lena Fisse[a], Jeremias Motte[a], Ralf Gold[a], and Kalliopi Pitarokoili[a]

Edited by Lawrence Steinman, Stanford University, Stanford, CA; received October 4, 2022; accepted December 15, 2022

In inflammatory neuropathies, oxidative stress results in neuronal and Schwann cell (SC) death promoting early neurodegeneration and clinical disability. Treatment with the short-chain fatty acid propionate showed a significant immunoregulatory and neuroprotective effect in multiple sclerosis patients. Similar effects have been described for patients with chronic inflammatory demyelinating polyneuropathy (CIDP). Therefore, Schwann cell's survival and dorsal root ganglia (DRG) outgrowth were evaluated in vitro after propionate treatment and application of H2O2 or S-nitroso-N-acetyl-D-L-penicillamine (SNAP) to evaluate neuroprotection. In addition, DRG resistance was evaluated by the application of oxidative stress by SNAP ex vivo after in vivo propionate treatment. Propionate treatment secondary to SNAP application on DRG served as a neuroregeneration model. Histone acetylation as well as expression of the free fatty acid receptor (FFAR) 2 and 3, histone deacetylases, neuroregeneration markers, and antioxidative mediators were investigated. β-hydroxybutyrate was used as a second FFAR3 ligand, and pertussis toxin was used as an FFAR3 antagonist. FFAR3, but not FFAR2, expression was evident on SC and DRG. Propionate-mediated activation of FFAR3 and histone 3 hyperacetylation resulted in increased catalase expression and increased resistance to oxidative stress. In addition, propionate treatment resulted in enhanced neuroregeneration with concomitant growth-associated protein 43 expression. We were able to demonstrate an antioxidative and neuroregenerative effect of propionate on SC and DRG mediated by FFAR3-induced histone acetylases expression. Our results describe a pathway to achieve neuroprotection/neuroregeneration relevant for patients with immune-mediated neuropathies.

FFAR3 | propionate | Schwann cells | dorsal root ganglia | chronic inflammatory demyelinating polyneuropathy

Significance

In inflammatory diseases of the peripheral nervous system, oxidative stress and neurodegeneration are the main factors resulting in long-term clinical disability. The fatty acid receptor 3 agonist propionate exerts a neuroprotective and neuroregenerative effect in the peripheral nervous system by histone acetylation. Our results describe a pathway to achieve neuroprotection for patients with immune-mediated neuropathies and have significant therapeutic implications for this group of patients.

In chronic inflammatory demyelinating polyradiculoneuropathy (CIDP), neuronal degeneration, including the apoptosis of myelinating Schwann cells (SCs), is primarily caused by autoimmune inflammation in the peripheral nervous system (PNS). However, mechanisms of degeneration secondary to neuroinflammation involve oxidative stress induced by reactive oxygen species (1–3). Oxidative stress is highly relevant in the pathophysiology of immune-mediated diseases of the PNS, as myelin is a vulnerable tissue due to its high lipid content (1). Since SCs are involved in immune regulation and are critical for neuronal nutrition and repair (4), secondary neurodegeneration is a main factor influencing disability in these diseases. None of the currently used drugs target oxidative stress or directly promote neuroregeneration.

Short-chain fatty acids (SCFAs), namely acetate, propionate (PA), and butyrate, are produced through dietary fiber fermentation by gut microbiota. Previous studies have shown that SCFAs modulate cell function by ligation to G protein-coupled free fatty acid receptor (FFAR) 2 and 3 and histone hyperacetylation by inhibiting histone deacetylases (HDAC) class I (5). Orally administered PA has shown antiinflammatory and neuroprotective potential in multiple sclerosis patients by increasing the frequency and activity of regulatory T cells, resulting in a reduction in relapse frequency and reduced brain atrophy (6, 7). Furthermore, there is anectotal evidence of a comparable beneficial effect of PA in the PNS, as shown in a case report of a patient with acute motor and sensory axonal neuropathy (8).

Here, we investigate and describe the antioxidative and neuroregenerative mechanisms of PA on SCs and dorsal root ganglia (DRGs) in vitro and ex vivo.

Results

Evidence of FFAR 3, but Not 2, in SCs and DRG at the Protein and mRNA Levels. Immunocytochemical staining was performed to investigate whether FFAR3 is expressed in SCs and DRGs. We were able to demonstrate perinuclear expression of FFAR3 in SCs and neurons (Fig. 1*A*). In addition to the immunohistochemical evidence, the expression

Competing interest statement: The authors have additional information to disclose. T.G. received compensation for activities with Biogen Idec. S.D. received compensation for activities with Sanofi Genzyme. A.H. has received speaker's fees from Bayer Healthcare, Biogen, Celgene, Genzyme, Merck, Novartis, and Teva. A.L.F. received research funding by Georgius Agricola Stiftung Ruhr; received honoraria and travel grants from Novartis AG, Sanofi, and Eisai GmbH, none related to this work; and owns shares of Fresenius SE & Co., Gilead Sciences, Medtronic PLC, and Novartis AG. J.M. received travel grants from Biogen Idec, Novartis AG, Teva, and Eisai GmbH, and his research is funded by Klaus Tschira Foundation and Ruhr-University, Bochum (FoRUM-program), none related to this work. R.G. received speaker's and board honoraria from Baxter, Bayer Schering, Biogen Idec, CLB Behring, Genzyme, Merck Serono, Novartis, Stendhal, Talecris, and TEVA, all not related to this manuscript. His department received grant support from Bayer Schering, BiogenIdec, Genzyme, Merck Serono, Novartis, and TEVA, all not related to this manuscript. K.P. received travel grants and speaker's honoraria from Biogen Idec and Bayer Schering, Novartis, and Grifols, all not related to this manuscript. All other authors have nothing to declare.

This article is a PNAS Direct Submission.

[1]To whom correspondence may be addressed. Email: Thomas.grueter@rub.de.

This article contains supporting information online at https://www.pnas.org/lookup/suppl/doi:10.1073/pnas.2216941120/-/DCSupplemental.

Published January 20, 2023.

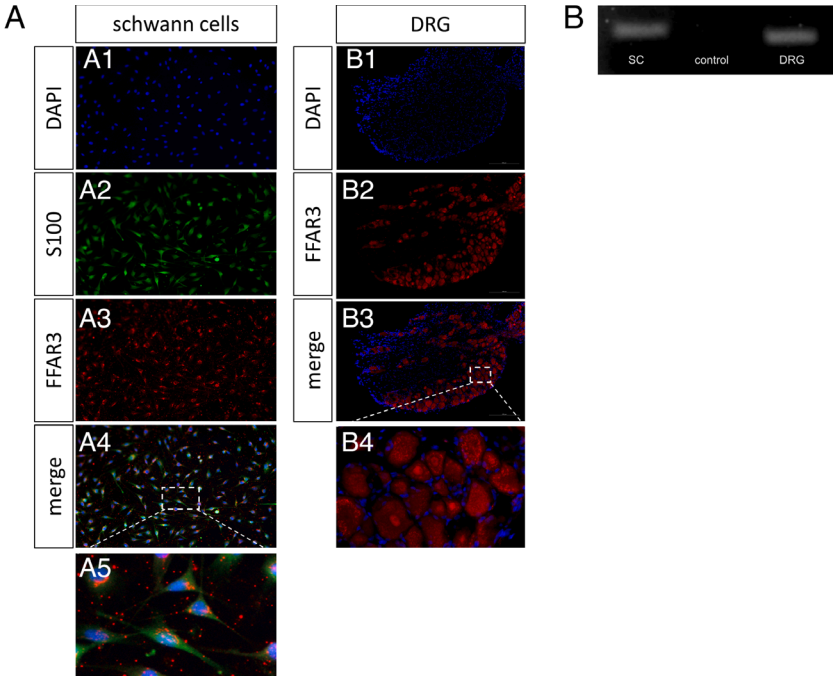

Fig. 1. Evidence of the free fatty acid receptor 3 on Schwann cells and dorsal root ganglia. The free fatty acid receptor 3 was evidence immunohistochemically (A) and on RNA level (B) in Schwann cells and dorsal root ganglia. (Scale bar, 50 μm.)

of FFAR3 in the SCs and DRGs was measured at the mRNA level (Fig. 1*B*).

Although FFAR2 has been detected in rodent intestinal cells, we were not able to demonstrate evidence of FFAR2 in either SCs or DRGs (*SI Appendix*, Fig. S1).

Propionate Increases the Resistance of SCs and DRG to Oxidative Stress by Catalase Expression. Flow cytometric analysis of propidium iodide (PI)-stained SCs was used to investigate the potential of PA to protect against H_2O_2-induced oxidative stress. Treatment of SCs with 0.03 mM H_2O_2 resulted in submaximal cell death, as shown by a 47.0 ± 9.1% PI-positive signal. Strikingly, simultaneous treatment with PA for 24 h significantly reduced cell death to 33.6 ± 9.6% on average compared to H_2O_2-treated SCs ($P < 0.0001$, n = 28, Fig. 2*A*). We were able to reproduce these results with the FFAR3 ligand β-hydroxybutyric acid (BHB): SCs treated simultaneously with H_2O_2 and BHB showed significantly restored cell viability (cell death: 28.7 ± 9.8%, $P < 0.0001$, n = 9, Fig. 2*A*). A combination of PA and BHB had the same effect as each substance administered separately (cell death: 37.2 ± 12.3%, $P = 0.0036$ in comparison to H_2O_2 alone, n = 9, Fig. 2*A*). Neither PA nor BHB showed any toxic effect on naive SCs when a concentration as high as 10 mM was used (*SI Appendix*, Fig. S2).

We detected a mean axonal outgrowth of 1,859 ± 362 μm in 24 h under naive conditions. However, there was no significant change in axonal outgrowth after PA treatment (Fig. 2*B*). Axonal outgrowth was significantly reduced by approximately 25.3% after induction of oxidative stress by S-nitroso-N-acetylpenicillamin (SNAP, $P = 0.0002$, n = 30, Fig. 2*B*). Twenty-four-hour PA pretreatment resulted in better outgrowth despite oxidative stress indicating a neuroprotective effect ($P = 0.03$, n = 16, Fig. 2*B*). We were able to abolish the neuroprotective effect of PA by simultaneous application of pertussis toxin (PTX, $P = 0.0394$, n = 13, Fig. 2*B*).

In order to transfer our in vitro results in an ex vivo concept, we orally treated rats with 150 mM propionate dissolved in 400 μL water or control gavaging for 5 d. After extraction, half of the DRGs of each group were exposed to oxidative stress. Only the DRGs of the control group showed a significant reduction of the axonal outgrowth after SNAP treatment ($P = 0.04$, n = 4, Fig. 2*C*).

Since PA increased resistance to oxidative stress in SCs and DRG, real-time PCR was performed to analyze the expression levels of antioxidants such as catalase, NAD(P)H quinone dehydrogenase 1 (NQO1), and heme oxygenase 1 (HO-1). Treatment with PA for 72 h significantly increased the relative expression of catalase mRNA by approximately 21.5% compared to naive SCs ($P = 0.0009$, n = 9, Fig. 2*D*), whereas the expression of catalase was also increased after 24 h of treatment but did not reach a level of significance. Similarly, catalase mRNA expression in DRGs was significantly increased after 24 h of PA treatment ($P = 0.007$, n = 6, Fig. 2*E*). No significant changes in the relative mRNA expression of HO-1 and NQO1 were shown after PA treatment (Fig. 2 *F* and *G*).

Propionate Induces Neuroregeneration by Growth Associated Protein 43 Expression. Propionate applied for 24 h on DRG after induction of oxidative stress by SNAP resulted in an increased outgrowth, indicating induction of neuroregeneration ($P = 0.0141$, n = 17, Fig. 3*A*). Consistently, PA treatment on naive DRG ($P < 0.0001$, n = 6, Fig. 3*B*) and on DRG after SNAP treatment ($P = 0.0026$, n = 5, Fig. 3*C*) resulted in increased expression of the plasticity protein growth associated protein 43 (gap-43).

β-hydroxybutyrate Treatment Results in Hyperacetylation of Histone 3 and 4 in SCs, whereas Propionate Leads Only to Hyperacetylation of Histone 3. Acetylation of histone 3 was increased 3.9-fold after 72 h of PA treatment compared to that in naive SCs ($P = 0.0002$, n = 6, Fig. 4*A*). After 24 h of PA treatment, we detected only a nonsignificant increase of approximately 1.5-fold compared to the control. In contrast to BHB treatment, PA treatment did not significantly alter the acetylation of histone 4. Acetylation of histone 3 lysine 9 (5.6-fold, $P < 0.0001$, n = 6, Fig. 4*A*) and histone 4 lysine 5 (16.9-fold, $P < 0.0001$, n = 6, Fig. 4*B*), lysine 8 (20.1-fold, $P < 0.0001$, n = 6, Fig. 4*C*), and lysine 16 (6.1-fold, $P < 0.0001$, n = 6, Fig. 4*E*), but not lysine 12 (Fig. 4D), were significantly increased after 24 h of BHB treatment.

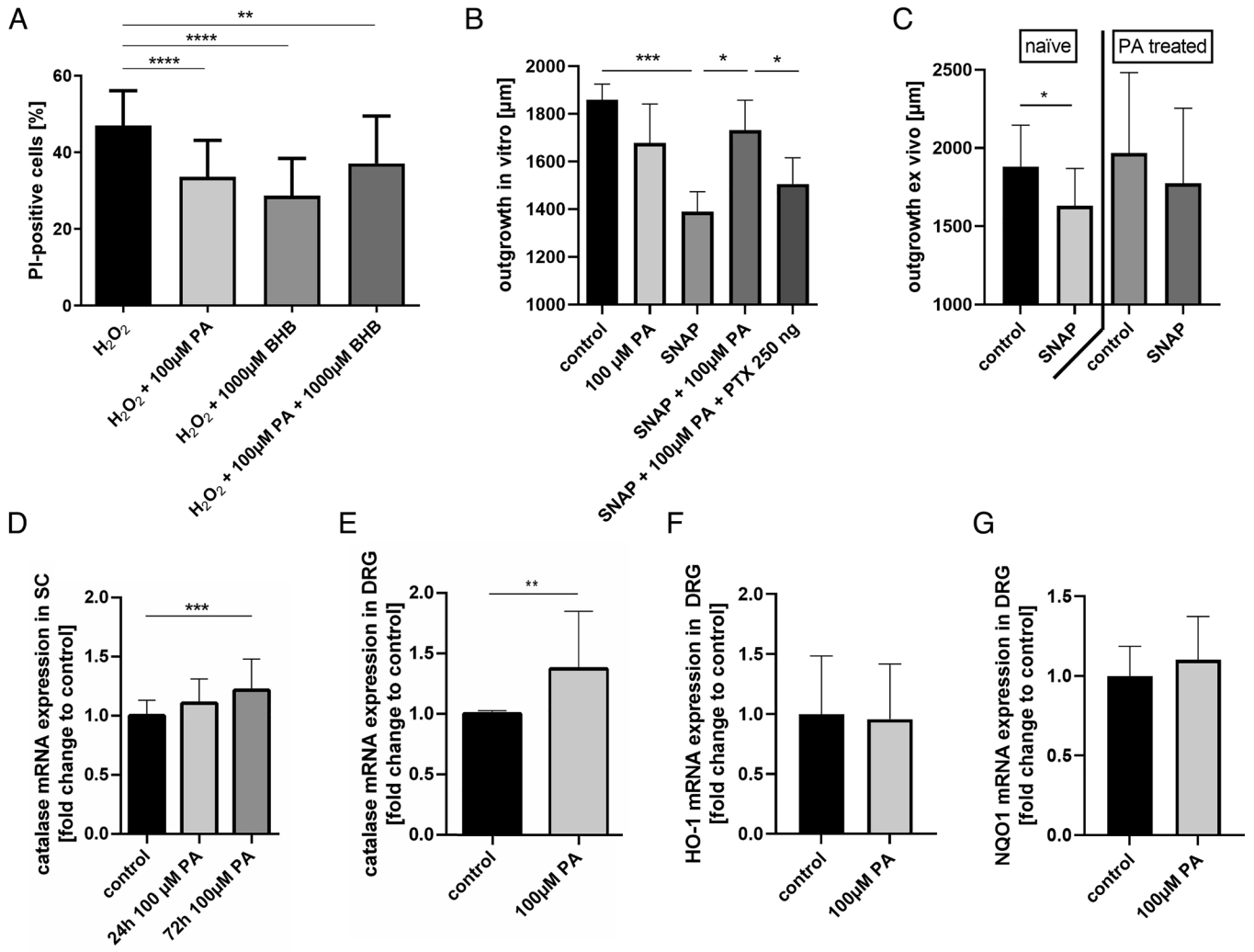

Fig. 2. The free fatty acid receptor 3 agonist propionate exerts neuroprotective effects on Schwann cells and dorsal root ganglia by increased catalase expression. Treatment of Schwann cells with both free fatty acid receptor 3 ligands, propionate or β-hydroxybutyrate, reduced H_2O_2 induced cell death significantly compared to control in flow cytometry (*A*). In line, pretreatment with propionate increased axonal outgrowth after SNAP application in comparison to control (*B*). Vice versa, addition of the G protein receptor inhibitor pertussis toxin abolished the neuroprotective effect of propionate in SNAP treated dorsal root ganglia (*B*). Similar, DRGs of control rats, but not propionate treated rats, showed a significantly reduction of axonal outgrowth after SNAP application (*C*). Propionate treatment of Schwann cells for 72 h significantly increased the relative expression of catalase compared to control (*D*), whereas the expression was also increased after 24-h treatment but did not reach the level of significance. In dorsal root ganglia, the catalase expression was increased 24 h after propionate treatment (*E*). No significant changes in the relative mRNA expression of HO-1 and NQO1 were shown after 24 h PA treatment in DRG (*F, G*). Data are provided as mean ± SD. $^*P < 0.05$, $^{**}P < 0.01$, $^{***}P < 0.001$, $^{****}P < 0.0001$.

Propionate Increases Histone Acetylation by Changing the Expression of Histone Deacetylase 2 and 8. The relative expression of HDAC 2 ($P = 0.02$, n = 9, Fig. 4*G*) was significantly reduced, by approximately 11.6%, and the expression of HDAC 8 ($P = 0.02$, n = 9, Fig. 4*I*) was increased by approximately 19.4% after PA treatment for 72 h. Treatment for 24 h resulted in a significant upregulation of HDAC 8 expression ($P = 0.048$, n = 9, Fig. 4*I*). The relative expression of HDAC 1 and HDAC 3 did not change after PA treatment for 24 h or 72 h (Fig. 4 *F–H*).

Discussion

We were able to demonstrate a neuroprotective and neuroregenerative effect of the FFAR3 agonist PA in the PNS in vitro. PA mediated an antioxidative effect in SCs and DRGs by downregulating HDAC 2 and upregulating HDAC 8 expression and subsequent hyperacetylation of histone 3, resulting in the upregulation of the major antioxidative enzyme catalase. Furthermore, PA treatment resulted in increased neuroregeneration after oxidative stress by gap-43 induction. The FFAR3 agonist BHB was able to mimic this effect, while the FFAR3 antagonist PTX abolished it.

Increasing incidence in autoimmune disorders in Western countries has been associated with alterations in gut microbiota and the daily intake of a diet low in fiber and enriched with refined carbohydrates (9). Since SCFAs, such as acetate, propionate, and butyrate, are produced by the fermentation of dietary fiber by gut microbiota, the presence of FFAR3 in the PNS may have an important physiological function in sensing nutritional status (10). There is evidence that the response of the extraintestinal system to available diary intake to maintain homeostasis is mediated by a gut-brain neural circuit via FFAR3 in peripheral nerves (11). Therefore, SCFAs regulate not only the body´s energy level but also inflammatory processes and antioxidative defense cascades (7, 9, 12–15). Similar to previous results demonstrating FFAR3 in the sympathetic ganglia (16) and the enteric nervous system (17), we provide evidence for the existence of FFAR3, but not FFAR2, in SCs and DRGs.

In contrast to the use of glucose and SCFA for dietary fiber fermentation by gut microbiota under conditions of adequate

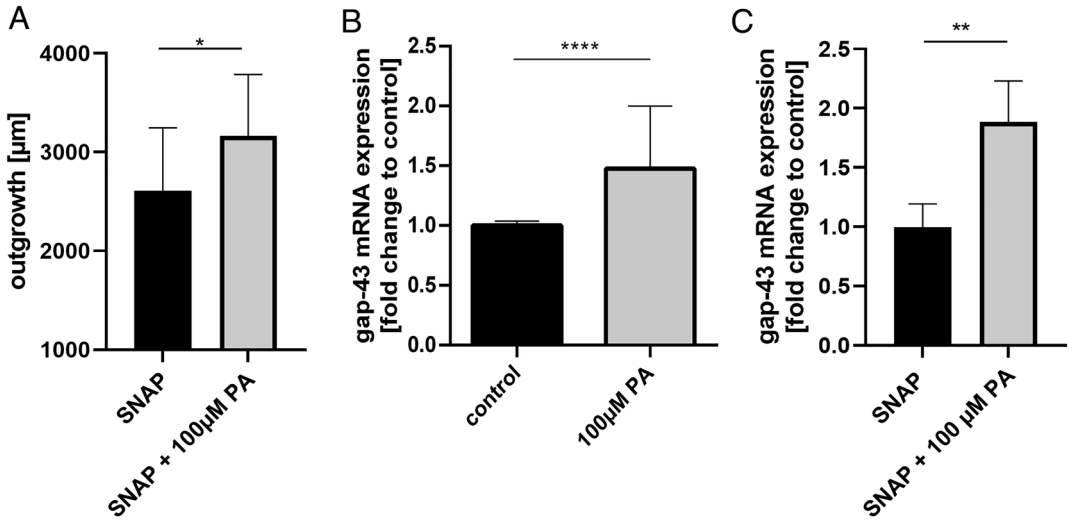

Fig. 3. Propionate exerts neuroregenerative effects by increased gap-43 expression. Propionate treatment resulted in an increased axonal outgrowth when applicated after SNAP administration (*A*). In line, propionate treatment resulted in an increased expression of the neuroregeneration marker growth associated protein 43 under naive conditions (*B*) and under oxidative stress mediated by SNAP (*C*). Data are provided as mean ± SD. **P* < 0.05, ***P* < 0.01, ****P* < 0.001, *****P* < 0.0001.

nutrition, ketone bodies, such as BHB, are produced in the liver during starvation or in diabetes. There are contradictory studies concerning the effects after BHB ligation to FFARs: Kimura et al. (16) reported an antagonistic effect of BHB on FFAR3 in sympathetic ganglia in mice, whereas Won et al. (18) demonstrated an agonistic effect in the rat sympathetic nervous system similar to our results. However, FFAR3 activation by SCFAs and ketone bodies might mediate different mechanisms and functions in various tissues and species due to high levels of posttranslational modification (9). In an experimental setting of glutamate- or H_2O_2-induced toxicity, BHB reduced the cell death rate and decreased the production of reactive oxygen species (19–21), comparable to our results in the PNS. Therefore, BHB and PA may induce neuroprotective mechanisms to restore balanced bioenergetic levels under starvation and fed conditions.

Histone modification in SC has an impact on development, PNS integrity, and resistance to injury (22). In this study, and in previous reports (23), PA was able to increase histone 3 acetylation by HDAC inhibition. The evidence that both FFAR3 ligands, BHB and PA, resulted in a comparable increase in resistance to oxidative stress by similar mechanisms and that the G protein inhibitor PTX abolished these effects is highly convincing for an

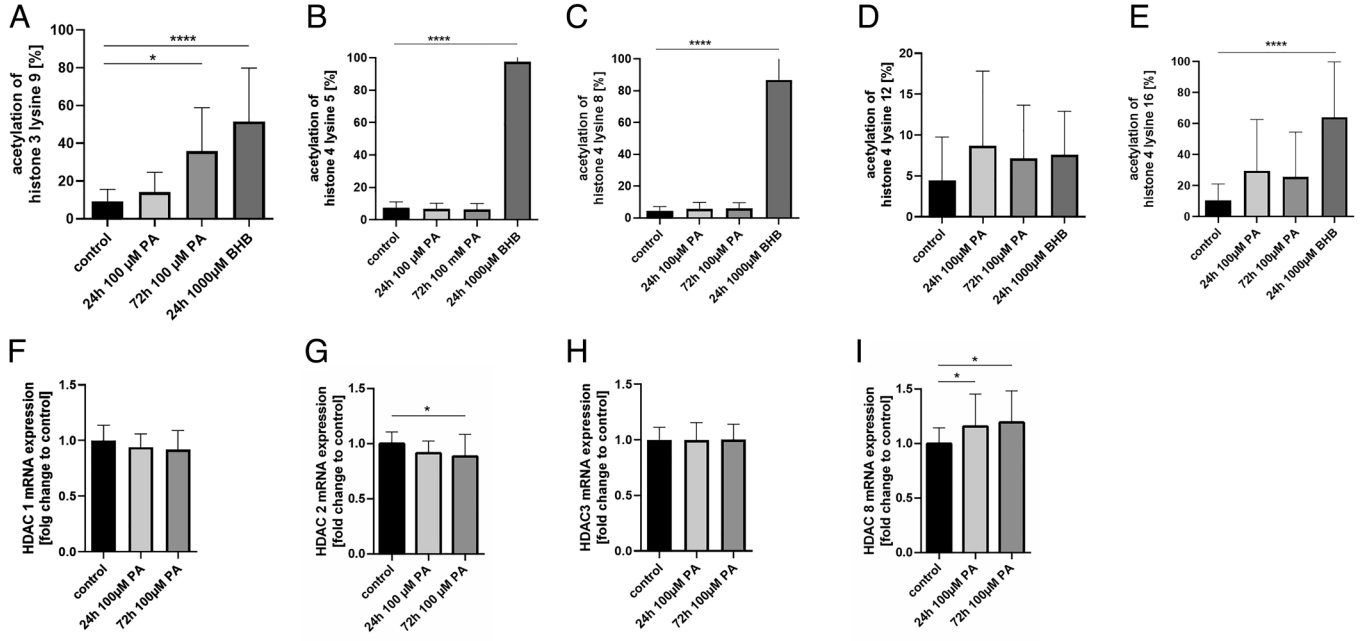

Fig. 4. Propionate treatment leads to histone hyperacetylation. Propionate treatment resulted in an increased acetylation of histone 3, but not histone 4. Acetylation of histone 3 lysine 9 (*A*) and histone 4 lysine 5 (*B*), lysine 8 (*C*), and lysine 16 (*E*), but not lysine 12 (*D*), were significantly increased after 24-h ß-hydroxybutyrate treatment. After propionate treatment, the relative expression of histone deacetylase 2 was significantly reduced (*G*) and the expression of histone deacetylase 8 was significantly increased (*I*) in Schwann cells. Treatment for 24 h resulted only in a nonsignificant trend for a reduction of HDAC 2 and 8. The relative expression of HDAC 1 and HDAC 3 did not change after PA treatment for 24 h or 72 h (*F*, *H*). Data are provided as mean ± SD. **P* < 0.05, ***P* < 0.01, ****P* < 0.001, *****P* < 0.0001.

FFAR3-mediated process. However, there is evidence for both PA and BHB being able to induce FFAR-independent HDAC inhibition (24). Irrespective of the mechanisms that induce HDAC inhibition, the resulting histone acetylation is a central step in PA-mediated pathways. PA exerts the greatest inhibition on class 1 HDACs, compromising HDAC 1, 2, 3, and 8. In contrast to previous assumptions, recent results have demonstrated a differing role for HDAC subtypes in preventing or promoting neurodegeneration (25). In the present study, we demonstrated a significant downregulation of HDAC 2 by PA treatment. Previous studies demonstrated that overexpression of HDAC 2 resulted in reduced dendritic spine density, synapse number, synaptic plasticity, and memory formation in mice (26). However, HDAC 2 also plays a distinct role in SC differentiation by regulating the key transcription factor Oct6: SCs appear in different forms, such as myelinating and repairing SCs (27). HDAC 2 activation increases myelination but impairs its differentiation into repair SCs (28), which is most important after cell damage, e.g., after injury or inflammation. Even though a balance between both states is probably essential, PA treatment may promote differentiation into repair SC and thereby increase resistance to oxidative stress. Further studies should be performed to clarify this issue.

Furthermore, we observed increased expression of HDAC 8. HDAC 8 overexpression has been proven in various cancer types (29), and it might regulate neural differentiation (30). However, the function of HDAC 8 is largely unknown (25).

Our results showing an antioxidative effect of PA in SCs and DRGs are in line with results obtained with nonneuronal cells (31–33). We demonstrated a direct neuroprotective effect of PA in the PNS by increased catalase expression following histone 3 acetylation. Catalase plays a central role in oxidative defense in autoimmune diseases and age-associated degeneration (34), and a dependency on histone 3 acetylation has been previously shown (35). Oxidative stress by itself induces an Nrf2-dependent antioxidative response in the DRG and increases the already high basal antioxidative enzyme expression in SCs (36). As PA induced a different antioxidative defense mechanism (catalase), both mechanisms might have complementary effects.

Inflammatory neuropathies are characterized by an inflammatory process and diminished antioxidative resistance and neuroregeneration (1, 37), resulting in demyelination and axonal damage. In a large cohort study of CIDP patients, severe axonal damage was evident already in patients at the time-point of first diagnosis, indicating oxidative stress and destruction of axonal integrity early in the disease course (38). We demonstrated increased viability after H_2O_2 or SNAP treatment, as well as increased expression of gap-43, a marker for neuroregeneration and plasticity in vitro. Hence, PA treatment in addition to first-line immunotherapy might be beneficial since it exerts antiinflammatory, (7) antioxidative, and neuroregenerative properties. This assumption is supported by reduced relapse rates and decreased brain atrophy after supplementation with SCFAs in multiple sclerosis patients (6) and a case report in which PA had an additional therapeutic effect in autoimmune inflammatory neuropathies (8). Therefore, our results reveal a neuroprotective and neuroregenerative treatment option and its mechanisms of action for immune-mediated neuropathies.

Materials and Methods

Animals. The present study was carried out in accordance with the European Communities Council Directive of September 22nd, 2010 (2010/63/EEC) for care of laboratory animals and after approval of the local government ethics committee (LANUV Recklinghausen, TVA 84-02.04.2017.A022). Male Sprague-Dawley rats (3 to 4 wk old, Charles River, RRID:RGD_1566457) were housed in a temperature- and humidity-controlled vivarium with a constant 12-h light/dark cycle (lights on from 6 a.m. to 6 p.m.) with ad libitum food and water access. All surgical procedures and experiments were conducted during the day.

Used Drugs. Sodium propionate (Sigma-Aldrich) was dissolved in water in a concentration of 100 μM. DL-β-hydroxybutyric acid (Sigma-Aldrich) was used as another FFAR3 ligand (16, 18) in a concentration of 1,000 μM dissolved in water. PTX was used as an FFAR3 antagonist in a concentration of 250 ng dissolved in water.

In Vivo Treatment with Propionate. First, 150 mM propionate was dissolved in water and 400 μL was administered twice daily for 5 d by oral gavage. Control received 400 μL water without propionate. The animals were randomly divided into both groups.

Isolation, Purification, and Cultivation of SCs. SCs were isolated as previously described (39, 40). In short, sciatic nerves were digested with dispase II (Sigma-Aldrich) and collagenase type I (Sigma-Aldrich) overnight. The resulting single-cell suspension was incubated for 5 d in a solution containing 2 μM forskolin (Sigma-Aldrich) and 10 nM neuregulin (PeproTech) to promote SC differentiation. After the separation of fibroblasts by magnetic cell selection, an SC purity above 95% was achieved. SC purity was controlled by FACS analysis with the SC marker SOX10 (1:1,000, rabbit recombinant monoclonal antibody, ab155279, RRID:AB_2650603, Abcam) after selection of viable cells (fixable viability dye eFlour 780, Thermo Fisher Scientific) as described by the manufacturer's protocol.

Isolation, Outgrowth, and Staining of DRG. DRGs were harvested and cultivated in a DRG growth medium as described previously (39). In short, single DRG explants were incubated in neurobasal medium (Invitrogen) containing 2% B27 (Life Technologies), 2% normal horse serum (Thermo Fischer Scientific), 1% l-glutamine (Thermo Fischer Scientific), 0.5% penicillin/streptomycin (Thermo Fischer Scientific), and 10 ng/mL neuronal growth factor (Sigma-Aldrich) at 37 °C and 5% CO_2. For immunohistochemical staining, DRGs were fixed with 4% paraformaldehyde (PFA) and incubated with blocking solution containing 10% goat serum and 0.05% Triton X-100. Afterward, the DRGs were incubated with the primary antibody βIII tubulin (1:7,500, T2200, RRID:AB_262133, Sigma-Aldrich) in blocking solution overnight. Appropriate secondary antibodies were used. To assess the explant outgrowth, lengths of the 10 longest neurites were measured with the NeuronJ® plugin (http://www.imagescience.org/meijering/software/neuronj/, RRID:SCR_002074).

Staining of the FFARs 2 on SCs. SCs transferred to coverslips coated with poly-l-lysine and laminin were fixed with 4% PFA for 10 min. A blocking solution containing 1% bovine serum albumin, 0.1% gelatin, 0.3 M glycine, 0.1 M phosphate buffer, and 10% normal goat serum with addition of 0.5% Triton X-100 was used. Polyclonal rabbit anti-FFAR2 antibody (1:250, orb159222, Biorbyt Ltd.) was used with an appropriate secondary antibody. Furthermore, nuclei were counterstained with 4′,6′-diamidino-2-phenylindole·2HCl (DAPI, Biozol Diagnostica Vertrieb). The omission of the primary antibodies served as negative control. The fluorescence signal in the rodent intestine was used as a positive control in regard to previous studies (41).

Costaining of the FFARs 3 and S100 on SCs. For immunocytochemical evidence of FFAR3 on SC in a costaining for the SC surface protein S-100, cells were transferred on poly-l-lysine- and laminin-coated coverslips. Cell processes were fixed by 4% PFA for 10 min. To achieve mild oxidation of the section, a treatment with 0.25% potassium permanganate and 5% oxalic acid was applied. Then, 1% bovine serum albumin, 0.1% gelatin, 0.3 M glycine, 0.1 M phosphate buffer, and 10% normal goat serum for 1 h at room temperature were used as blocking solution. Polyclonal rabbit anti-FFAR3 antibody (1:50, PA5-75521, RRID:AB_2719249, Thermo Fisher Scientific) and monoclonal mouse S-100 antibody (1:300, MABO79-1, Merck) were used with their appropriate secondary antibody. Nuclei were counterstained with DAPI. The omission of the primary antibodies served as negative control. Specificity of S-100 staining was also controlled on sections of fibroblasts.

Confirmation of the Evidence of the FFAR 3 in SCs and DRG on RNA Level. To investigate FFAR3 mRNA-expression in SC and DRG, sequence-specific sense- and antisense-primers were designed (sen GGA GGG GTG TGG AAA ACA CT, ase GGA ACA ACC TGC AGA CGA AG). The PCR was performed with the Promega Accustart® system with the following amplification protocol: 94 °C for 3 min

(initial denaturation), followed by 34 cycles of 94 °C for 30 s, 60 °C for 30 s, and 72 °C for 30 s, before a final elongation at 72 °C for 5 min was performed. Analysis of the PCR products was accomplished by electrophoresis. SC and DRG samples were loaded onto a 2% agarose gel prepared with 1×-TAE buffer and 5% Roti-gel stain for the visualization of DNA fragments.

Staining of the FFARs 2 and 3 on DRG. DRGs were fixed with 4% PFA and placed in 30% sucrose. DRGs were embedded in Tissue-Tek O.C.T cryomedium and cut into 10-µm slices using a microtome HM 550 cryostat (Thermo Fisher Scientific). DRG sections were cooked in 100 mM citrate buffer for 10 min and blocked with 10% goat serum and 0.5% Triton X-100. Primary antibodies for FFAR2 (orb159222, Biorbyt Ltd.) or FFAR3 (PA5-75521, Thermo Fisher Scientific) were diluted 1:100 in blocking solution and incubated overnight. Sections were incubated with an appropriate secondary antibody and mounted with Fluoromount with DAPI.

Application of Oxidative Stress on SCs. To investigate if PA reduces oxidative stress in SCs and to analyze whether BHB acts in an agonistic or antagonistic way on FFAR3, SC were treated with 0.03 mM H_2O_2 for 24 h with or without PA and/or BHB treatment simultaneously. The resistance of SC to oxidative stress was determined by the percentage of PI-positive cells in flow cytometry indicating cell death. The concentration of H_2O_2 to generate a submaximal stress level as well as labeling protocol was determined previously (39, 40).

Neuroprotection against Oxidative Stress in DRG. DRG explants were cultivated for 24 h in a DRG growth medium containing 100 µM PA treatment, 100 µM PA, and 250 ng PTX treatment or Aqua dest. as control. The medium was replaced by 2 mM SNAP in a fresh DRG growth medium to induce oxidative stress. Thereafter, DRG explants were fixed with 4% PFA and stained for βIII tubulin, and neurite outgrowth was assessed as described above.

Induction of Neuroregeneration after Oxidative Stress in DRG. DRG explants were cultivated for 24 h in a DRG growth medium. The medium was replaced by 2 mM SNAP in a fresh DRG growth medium for 24 h to induce oxidative stress. Thereafter, the medium was replaced by DRG growth medium containing 100 µM PA treatment or Aqua dest. as control. Thereafter, DRG explants were fixed with 4% PFA and stained for βIII tubulin, and neurite outgrowth was assessed as described above.

Analyzing the Effect of Propionate on SCs and DRG on the mRNA Level. In order to detect whether PA regulates the transcription of FFAR3, antioxidant proteins, neuronal regeneration markers, and HDACs, real-time PCR was performed with naive and 24-h and 72-h PA-treated SC and DRGs. For analyzing the plasticity protein gap-43, DRGs were also analyzed after SNAP application with or without 24-h PA treatment. The procedure is described elsewhere (39, 40). In short, total RNA was isolated using the RNeasy Mini extraction kit (Qiagen, Naamloze, Netherlands). All samples were treated with the RNA Stabilization Reagent (RNAlater, Qiagen) at 37 °C overnight and stored at −80 °C until use. Total RNA was transcribed into cDNA as described by the manufacturer's protocol for the Reverse Transcription System (Promega). The following sequence-specific sense (sen) and antisense (ase) primers were designed, and mRNA expression levels were analyzed by quantitative rt-PCR according to the manufacturer's instructions (Thermo Fisher Scientific): ß-actin (sen CCC ATC TAT GAG GGT TAC GC, ase TTT AAT GTC ACG CAC GAT TTC), glyceraldehyde 3-phosphate dehydrogenase (GAPDH, sen AGG TCA CCC AGA GCT GAA CG, ase CAC CCT GTT GCT GTA GCC GTA T), FFAR3 (sen GGA GGG GTG TGG AAA ACA CT, ase GGA ACA ACC TGC AGA CGA AG), Catalase (sen CGG CAC ATG AAT GGC TAT GG, ase TGC CCT GGT CAG TCT TGT AAT), HO-1 (sen AGG AAA ATC CCA GAT CAG CAG, ase GAA AAG AGA GCC AGG CAA GAT), NQO1 (sen GTT TCT TTT TCC CCA GTT TGC, ase GGC TAC ACC TCT CCC TGA TTC), gap-43 (sen CTC TCC TGC CCT TTC TCA GAT, ase ACT CGC CAT AAC AAC AAC AAG), HDAC 1 (sen CAG AAG CCA AAG GGG TCA AAG, ase TGA GGG AAA GTA AGG GAC TTG G), HDAC 2 (sen GCG GCA AGA AGA AAG TGT GC, ase CAT CCG GAT CCT ATG GGG CT), HDAC 3 (sen CTA TGA CAG GAC TGA CGA GGC, ase CCT TGT CAT TGT CAT GGT CTC C), and HDAC 8 (sen AGA TCC CAG ATC ATG AGT TTT TCA C, ase ACC ACA TGC TTC AGA TTC CCT). Relative target mRNA expression was normalized to the geometric expression average of the housekeeping genes β-actin and GAPDH. We applied each sample in three technical replicates. The mean Ct was used in the equation for the housekeeping genes and Ct for the genes of interest.

Analyzing the Effect of Propionate and β-Hydroxybutyrate on Acetylated Histones 3 and 4 in SCs. To detect whether PA or BHB increases histone acetylation, immunohistochemical staining was performed with naive, PA-, or BHB-treated SC for 24 and 72 h. SCs, that were transferred on poly-l-lysine- and laminin-coated coverslips, were fixed by 4% PFA for 10 min and permeabilized with 0.3% Triton-X for 3 min. A blocking solution containing 5% bovine serum albumin was used. The following primary antibodies were used: rabbit polyclonal antibody against acetylated histone 3 lysine 9 (1 µg/mL, ab10812, RRID:AB_297491, Abcam) and against acetylated histone 4 lysine 5 (1:1,000), 8 (1:500), 12 (1:500), and 16 (1:500) from Merck (17-211, RRID:AB_390248). Appropriate secondary antibodies were used. Nuclei were counterstained with DAPI. The omission of the primary antibodies served as negative control. For statistical analysis, nuclei with an intensive fluorescence signal for each histone marker have been counted in relation to all DAPI-positive cells in a blinded fashion. Three different areas were analyzed per coverslip.

Statistics. Statistical analyses were performed by GraphPad Prism 7 software (GraphPad Software Inc., http://www.graphpad.com/, RRID:SCR_002798). Data are provided as mean ± SD. Differences between pairs of groups were tested by Student's *t* test if normally distributed and the Mann–Whitney *t* test if not normally distributed. Differences between three or more groups were tested by ANOVA if normally distributed and the Kruskal–Wallis test if not normally distributed. The Shapiro–Wilk test was used to test for normal distribution. For all analyses, the statistically significant threshold was set at a probability value <0.05, and their levels are indicated as * = $P < 0.05$, ** = $P < 0.01$, *** = $P < 0.001$, and **** = $P < 0.0001$.

Data, Materials, and Software Availability. All study data are included in the article and/or *SI Appendix*.

ACKNOWLEDGMENTS. The authors have not declared a specific grant for this research from any funding agency in the public, commercial or not-for-profit sectors.

Author affiliations: [a]Department of Neurology, St. Josef Hospital, Ruhr University Bochum, 44791 Bochum, Germany; and [b]Department of Neurology, Otto-von-Guericke University, 39120 Magdeburg, Germany

Author contributions: T.G. and K.P. designed research; T.G., N.M., N.R., A.B., M.S., S.D., X.P., and K.L. performed research; T.G., N.M., N.R., and A.B. analyzed data; T.P., N.R., A.B., M.S., B.G., A.H., A.L.F., J.M., R.G., and K.P. revised the paper; and T.G. wrote the paper.

1. G. Marrali *et al.*, NADPH oxidase 2 (NOX2) enzyme activation in patients with chronic inflammatory demyelinating polyneuropathy. *Eur. J. Neurol.* **23**, 958–963 (2016).
2. N. Mossberg *et al.*, Leukocyte oxygen radical production determines disease severity in the recurrent Guillain-Barré syndrome. *J. Inflamm. (Lond).* **7**, 40 (2010).
3. T. Kawasaki *et al.*, Up-regulation of cyclooxygenase-2 in inflammatory demyelinating neuropathy. *Acta Neuropathol.* **101**, 154–158 (2001).
4. G. M. Z. Horste *et al.*, Expression of antigen processing and presenting molecules by Schwann cells in inflammatory neuropathies. *Glia* **58**, 80–92 (2010).
5. M. G. Rooks, W. S. Garrett, Gut microbiota, metabolites and host immunity. *Nat. Rev. Immunol.* **16**, 341–352 (2016).
6. A. Duscha *et al.*, Propionic acid shapes the multiple sclerosis disease course by an immunomodulatory mechanism. *Cell* **180**, 1067–1080.e16 (2020).
7. A. Haghikia *et al.*, Dietary fatty acids directly impact central nervous system autoimmunity via the small intestine. *Immunity* **43**, 817–829 (2015).
8. M.-S. Yoon *et al.*, Treatment of an acute motor and sensory axonal neuropathy with propionate in a 33-year-old male. *Ther. Adv. Neurol. Disord.* **11**, 1756286418809580 (2018).
9. S. Sivaprakasam, P. D. Prasad, N. Singh, Benefits of short-chain fatty acids and their receptors in inflammation and carcinogenesis. *Pharmacol. Ther.* **164**, 144–151 (2016).
10. A. Ichimura, S. Hasegawa, M. Kasubuchi, I. Kimura, Free fatty acid receptors as therapeutic targets for the treatment of diabetes. *Front. Pharmacol.* **5**, 236 (2014).
11. F. de Vadder *et al.*, Microbiota-generated metabolites promote metabolic benefits via gut-brain neural circuits. *Cell* **156**, 84–96 (2014).
12. E. Ansaldo, T. K. Farley, Y. Belkaid, Control of immunity by the microbiota. *Annu. Rev. Immunol.* **39**, 449–479 (2021).
13. H. C. Wastyk *et al.*, Gut-microbiota-targeted diets modulate human immune status. *Cell* **184**, 4137–4153.e14 (2021).
14. M. E. Perez-Muñoz *et al.*, Nutritional and ecological perspectives of the interrelationships between diet and the gut microbiome in multiple sclerosis: Insights from marmosets. *iScience* **24**, 102709 (2021).
15. R. R. Bonomo *et al.*, Fecal transplantation and butyrate improve neuropathic pain, modify immune cell profile, and gene expression in the PNS of obese mice. *Proc. Natl. Acad. Sci. U.S.A.* **117**, 26482–26493 (2020).

16. I. Kimura *et al.*, Short-chain fatty acids and ketones directly regulate sympathetic nervous system via G protein-coupled receptor 41 (GPR41). *Proc. Natl. Acad. Sci. U.S.A.* **108**, 8030–8035 (2011).
17. M. K. Nøhr *et al.*, GPR41/FFAR3 and GPR43/FFAR2 as cosensors for short-chain fatty acids in enteroendocrine cells vs FFAR3 in enteric neurons and FFAR2 in enteric leukocytes. *Endocrinology* **154**, 3552–3564 (2013).
18. Y.-J. Won, B. van Lu, H. L. Puhl, S. R. Ikeda, β-Hydroxybutyrate modulates N-type calcium channels in rat sympathetic neurons by acting as an agonist for the G-protein-coupled receptor FFA3. *J. Neurosci.* **33**, 19314–19325 (2013).
19. M. Maalouf, P. G. Sullivan, L. Davis, D. Y. Kim, J. M. Rho, Ketones inhibit mitochondrial production of reactive oxygen species production following glutamate excitotoxicity by increasing NADH oxidation. *Neuroscience* **145**, 256–264 (2007).
20. M. Nagao *et al.*, β-Hydroxybutyrate elevation as a compensatory response against oxidative stress in cardiomyocytes. *Biochem. Biophys. Res. Commun.* **475**, 322–328 (2016).
21. T. Shimazu *et al.*, Suppression of oxidative stress by β-hydroxybutyrate, an endogenous histone deacetylase inhibitor. *Science* **339**, 211–214 (2013).
22. M. Duman, M. Martinez-Moreno, C. Jacob, N. Tapinos, Functions of histone modifications and histone modifiers in Schwann cells. *Glia* **68**, 1584–1595 (2020).
23. M. Kobayashi *et al.*, A short-chain fatty acid, propionate, enhances the cytotoxic effect of cisplatin by modulating GPR41 signaling pathways in HepG2 cells. *Oncotarget* **9**, 31342–31354 (2018).
24. M. Li, B. C. A. M. van Esch, P. A. J. Henricks, G. Folkerts, J. Garssen, The anti-inflammatory effects of short chain fatty acids on lipopolysaccharide- or tumor necrosis factor α-stimulated endothelial cells via activation of GPR41/43 and inhibition of HDACs. *Front. Pharmacol.* **9**, 533 (2018).
25. E. A. Thomas, S. R. D'Mello, Complex neuroprotective and neurotoxic effects of histone deacetylases. *J. Neurochem.* **145**, 96–110 (2018).
26. J.-S. Guan *et al.*, HDAC2 negatively regulates memory formation and synaptic plasticity. *Nature* **459**, 55–60 (2009).
27. K. R. Jessen, R. Mirsky, The repair Schwann cell and its function in regenerating nerves. *J. Physiol.* **594**, 3521–3531 (2016).
28. V. Brügger *et al.*, Delaying histone deacetylase response to injury accelerates conversion into repair Schwann cells and nerve regeneration. *Nat. Commun.* **8**, 14272 (2017).
29. N. Adhikari, S. A. Amin, T. Jha, Selective and nonselective HDAC8 inhibitors: A therapeutic patent review. *Pharm. Pat. Anal.* **7**, 259–276 (2018).
30. S. Katayama *et al.*, HDAC8 regulates neural differentiation through embryoid body formation in P19 cells. *Biochem. Biophys. Res. Commun.* **498**, 45–51 (2018).
31. A. Filippone *et al.*, The anti-inflammatory and antioxidant effects of sodium propionate. *Int. J. Mol. Sci.* **21**, 3026 (2020).
32. W. Huang *et al.*, Short-chain fatty acids ameliorate diabetic nephropathy via GPR43-mediated inhibition of oxidative stress and NF-κB signaling. *Oxid. Med. Cell. Longev.* **2020**, 4074832 (2020).
33. L.-C. Tong *et al.*, Propionate ameliorates dextran sodium sulfate-induced colitis by improving intestinal barrier function and reducing inflammation and oxidative stress. *Front. Pharmacol.* **7**, 253 (2016).
34. A. Nandi, L.-J. Yan, C. K. Jana, N. Das, Role of catalase in oxidative stress- and age-associated degenerative diseases. *Oxid. Med. Cell Longev.* **2019**, 9613090 (2019).
35. T.-B. Lee, Y.-S. Moon, C.-H. Choi, Histone H4 deacetylation down-regulates catalase gene expression in doxorubicin-resistant AML subline. *Cell Biol. Toxicol.* **28**, 11–18 (2012).
36. A. M. Vincent, K. Kato, L. L. McLean, M. E. Soules, E. L. Feldman, Sensory neurons and schwann cells respond to oxidative stress by increasing antioxidant defense mechanisms. *Antioxid. Redox Signal.* **11**, 425–438 (2009).
37. H.-Y. Tang *et al.*, Alterations of plasma concentrations of lipophilic antioxidants are associated with Guillain-Barre syndrome. *Clin. Chim. Acta* **470**, 75–80 (2017).
38. T. Grüter *et al.*, Pathological spontaneous activity as a prognostic marker in chronic inflammatory demyelinating polyneuropathy. *Eur. J. Neurol.* **27**, 2595–2603 (2020).
39. T. Grüter *et al.*, Immunomodulatory and anti-oxidative effect of the direct TRPV1 receptor agonist capsaicin on Schwann cells. *J. Neuroinflammation* **17**, 145 (2020).
40. K. Pitarokoili *et al.*, Intrathecal triamcinolone acetonide exerts anti-inflammatory effects on Lewis rat experimental autoimmune neuritis and direct anti-oxidative effects on Schwann cells. *J. Neuroinflammation* **16**, 58 (2019).
41. E. Le Poul *et al.*, Functional characterization of human receptors for short chain fatty acids and their role in polymorphonuclear cell activation. *J. Biol. Chem.* **278**, 25481–25489 (2003).